Nano Res (2009) 2: 671–677
DOI 10.1007/s12274-009-9070-3
Research Article

Magnetoresistance Oscillations of Ultrathin Pb Bridges

Jian Wang[1, 2] (✉), Xucun Ma[1], Shuaihua Ji[1], Yun Qi[1], Yingshuang Fu[1], Aizi Jin[1], Li Lu[1], Changzhi Gu[1], X. C. Xie[1, 3], Mingliang Tian[2], Jinfeng Jia[1, 4], and Qikun Xue[1, 4] (✉)

[1] Institute of Physics, Chinese Academy of Sciences, Beijing 100190, China
[2] The Center for Nanoscale Science and Department of Physics, The Pennsylvania State University, University Park, Pennsylvania 16802-6300, USA
[3] Department of Physics, Oklahoma State University, Stillwater, OK 74078, USA
[4] Department of Physics, Tsinghua University, Beijing 100084, China

Received: 11 May 2009 / Revised: 18 June 2009 / Accepted: 30 June 2009

ABSTRACT

Pb nanobridges with a thickness of less than 10 nm and a width of several hundred nm have been fabricated from single-crystalline Pb films using low-temperature molecular beam epitaxy and focus ion beam microfabrication techniques. We observed novel magnetoresistance oscillations below the superconducting transition temperature (T_C) of the bridges. The oscillations—which were not seen in the crystalline Pb films—may originate from the inhomogeneity of superconductivity induced by the applied magnetic fields on approaching the normal state, or the degradation of film quality by thermal evolution.

KEYWORDS

Pb nanobridge, magnetoresistance, superconductivity, molecular beam epitaxy, scanning tunneling microscope, focus ion beam

Introduction

With the rapid development of nanotechnology, superconductivity in quasi-one-dimensional (quasi-1-D) nanowires and quasi-two-dimensional (quasi-2-D) films has attracted considerable attention [1–18]. Many interesting physical phenomena—such as dissipations caused by thermally activated phase-slips or quantum phase-slips, multiple voltage steps in the voltage–current (V–I) characteristics due to phase-slip centers [19, 20], and elevated superconducting transition temperatures (T_C) [20, 21]—have been observed in quasi-1-D superconductors. For quasi-2-D ultrathin crystalline Pb films, oscillatory superconductivity modulated by quantum size effects was recently reported [11–15]. On this basis, some interesting superconductivity behavior would be expected in a system intermediate between quasi-1-D and quasi-2-D superconductors.

In an earlier study, we studied the superconductivity in a 28 atomic monolayers (ML) thick, 285 nm wide, and 10 μm long crystalline Pb bridge [22]. Since the superconducting coherence length in a Pb film of 28 ML (~8 nm) thickness is ~27 nm, the 285 nm wide Pb nanobelt having the same thickness can be considered as a superconductor with

Address correspondence to Jian Wang, juw17@psu.edu; Qikun Xue, qkxue@mail.tsinghua.edu.cn

dimensions between 2-D and quasi-1-D. In this work, we focus on the magnetoresistance (MR) oscillations in such Pb nanobridges. The oscillations are similar to those reported in 1-D amorphous and granular superconducting nanowires [23, 24]. Because our nanobridges were made from high-quality single-crystal Pb films fabricated by low-temperature molecular beam epitaxy, the observation of such MR oscillations in these crystalline Pb nanobridges is quite unexpected. In order to elucidate the possible mechanisms of these interesting oscillations, in this work we carried out a systematic study of a series of Pb nanobridge samples with different dimensions. It was found that the oscillations were seen only in nanobridges and not in the crystalline Pb films, indicating that they may originate from the inhomogeneity of superconductivity in the bridges.

1. Experimental

High quality single-crystal Pb films were grown on high resistive Si (111) substrates [11] in an ultra-high vacuum low-temperature scanning tunneling microscopy (STM) system integrated with a molecular beam epitaxy (MBE) chamber (Unisoku USM-1300). The base pressure of the system is better than 1.0×10^{-10} Torr. Clean Si (111)-7 × 7 surfaces with terraces of more than 100 nm in width on average were obtained by high temperature flashing at 1200 °C for several seconds. To achieve atomically flat crystalline Pb thin films over a macroscopic area, the Si substrates were cooled down to ~95 K by liquid nitrogen during growth, as reported elsewhere [22]. Pb with a purity of 99.999% was evaporated onto the Si substrates from a pyrolytic boron nitride (PBN) Knudsen cell at a flux rate of 0.32 ML/min in the MBE chamber. A reflection high-energy electron diffraction (SPECS RHD-30) setup was used to monitor the growth and to calibrate the deposition rates. All STM topographic images were recorded at 80 K with a constant current of 100 pA.

Figure 1(a) shows a typical STM topographic image of a Pb film with a thickness of 30 ML, and clearly reveals the atomically smooth nature of the film prepared by this method. Steps of one ML in height seen on the image are a reflection of the Si(111) substrate steps. To fabricate bridges from the films, the films were covered with 4 ML Au as a protective layer [11, 14] and were then transferred out of the UHV growth chamber. The bridges were carved from the films by a commercial focused ion beam etching and depositing system (FEI-DB235), as shown schematically in Fig. 1(b). The etching current was set less than 10 pA in order to minimize contamination and structure damage by the Ga ions. Four bridges of different dimensions (length × width × thickness) were made: sample #1: 2 μm × 350 nm × 30 ML, sample #2: 2 μm × 350 nm × 23 ML, sample #3: 2 μm × 350 nm × 29 ML and sample #4: 10 μm × 284 nm × 28 ML. Four Au wires of 25 μm in diameter were pressed onto the surface of the two parts of the film with indium for transport measurements with a Physical Property Measurement System (Quantum Design Model 6000).

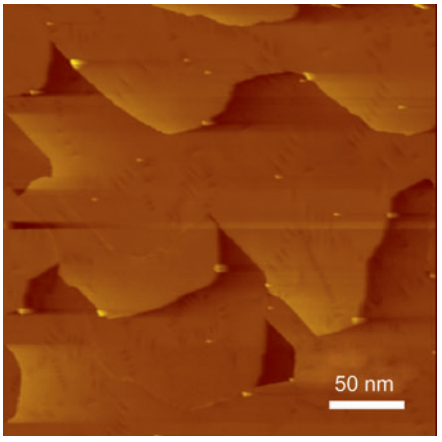

(a)

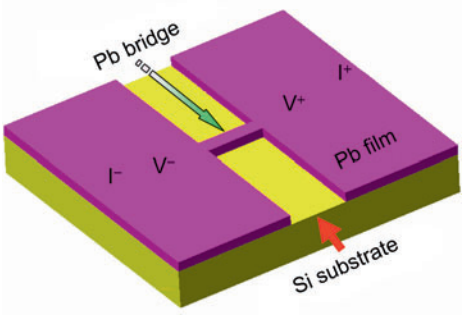

(b)

Figure 1 (a) A scanning tunneling microscope image of the 30 ML atomically flat Pb thin film on the Si(111)-7 × 7 substrate. The image was recorded at 80 K with a constant current of 100 pA. (b) A schematic view of the fabrication of a bridge from the film in (a) and the transport measurement across the Pb bridge

2. Results and discussion

Figure 2 shows the resistance vs. temperature (R–T) curves of samples #1, #2, and #3, measured with a default excitation current of 50 nA. Each curve was normalized to its normal state resistance (R_0) at 8 K with $R_0^{\#1}$ = 612 Ω, $R_0^{\#2}$ =1476 Ω, and $R_0^{\#3}$= 4835 Ω. The inset is a scanning electron microscope image of sample #1. The interesting result here is that samples #1 and #2 show almost zero resistance below T_C, whereas in contrast sample #3 exhibits a large finite residual resistance down to 2.0 K. Since all three bridges were fabricated with the exact same conditions during the FIB processing, destruction or contamination by FIB processing cannot be the reason for this large finite resistance. Most likely it is due to the degradation of the film in air, because this sample was exposed in air at room temperature for a few days before cooling down to helium temperature for measurement (samples #1 and #2 were measured immediately after the bridges were fabricated from the films).

The resistance of sample #1 as a function of the magnetic field (H) applied perpendicularly to the film at 2 K is shown in Fig. 3(a). The magnetic field-induced transition region is much wider than that of the Pb films [14, 22]. Figure 3(b) is a magnified

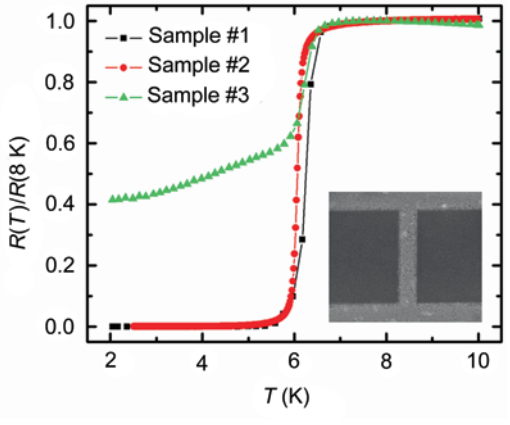

Figure 2 Resistance as a function of temperature measured for samples #1, #2, and #3. The inset is a typical scanning electron micrograph of the Pb bridge, which was made from the single-crystal Pb film. The Pb bridge is 350 nm in width and 2 μm in length. The dark regions on the two sides of the Pb bridge are the exposed Si substrate, which isolates two blocks of the Pb film

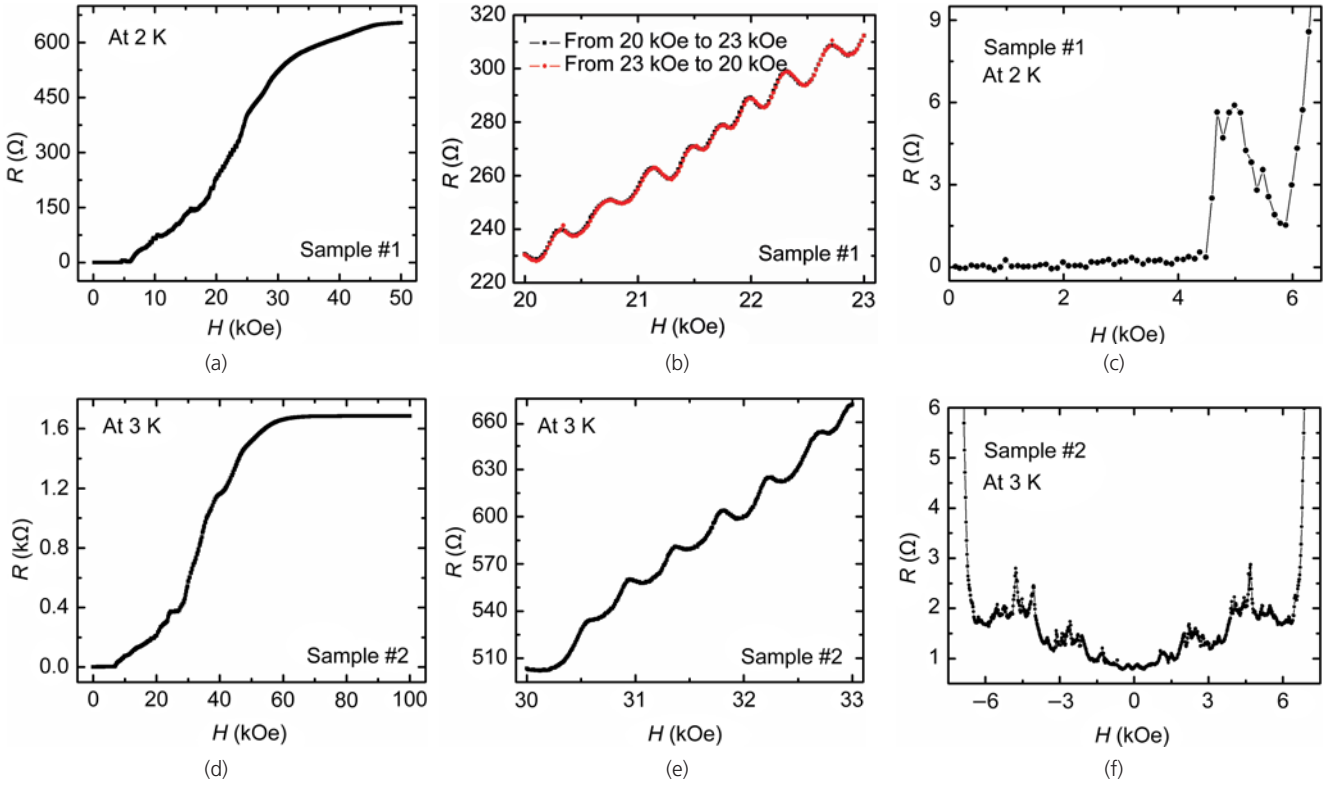

Figure 3 (a) Magnetoresistance of sample #1 with a magnetic field applied perpendicular to the film at 2 K; (b) close-up view of (a) from 20 to 23 kOe for clarity; (c) magnetoresistance of sample #1 in the low field regime at 2 K; (d) magnetoresistance of sample #2 with a magnetic field applied perpendicular to the film at 3 K; (e) close-up view of (d) from 30 to 33 kOe for clarity; (f) magnetoresistance of sample #2 in the low field regime at 3 K

view of Fig. 3(a) from 20 to 23 kOe (in the transition region). A quasi-periodic MR oscillation with a period of ~394 Oe is evident. The oscillations are reproducible and no hysteresis was seen in cycles of sweeping up and down the field. Figure 3(c) is a close-up view of Fig. 3(a) in the low field regime. Zero resistance was observed below 4 kOe. Figures 3 (d), 3(e), and 3(f) show the R–H behaviour of sample #2 for comparison. Despite the thickness difference (sample #2 is 23 ML thick and sample #1 is 30 ML thick), the R–H curves of sample #2 are similar to those of sample #1 (see Fig. 3(a) and Fig. 3(d)). The quasi-periodic oscillations were also observed in sample #2 (Fig. 3(e)) with a period of about 428 Oe at 3 K. However, sample #2 showed a finite resistance of ~0.8 Ω even at zero field and non-periodic oscillations were observed in the low field regime (Fig. 3(f)). The oscillations were symmetric for opposing perpendicular fields.

Interestingly, strong MR oscillations were found in sample #3 with large finite residual resistance (see Fig. 4(a)). The oscillations were observed from zero field to the transition region. Below T_C, the oscillation amplitude became smaller with increasing temperature. Nevertheless, the field positions of the oscillations were independent of the temperature in the low field regime. Figure 4(b) is a close-up view of the R–H curve at 2.5 K at low field. In this case, the oscillations disappear when the field is larger than 26 kOe and the period of the quasi-periodic oscillations is about 849 Oe, although it is not very well-defined. Sample #3 also showed a slight enhancement of resistance with decreasing temperature (see Fig. 2) in the temperature range above T_C, and a small negative MR in R–H curves above the critical field H_C. This phenomenon is reminiscent of "granular" behavior in superconducting nanowires.

We emphasize that none of the quasi-periodic oscillations found in the bridge samples were seen in any of the original single-crystal 2-D thin films. Further evidence was seen in sample #4 (Fig.5), which has dimensions of 10 μm × 284 nm × 28 ML and a large finite residual resistance below T_C. Figure 5(a) shows R–T curves of the 28 ML thick film and nanobridge sample #4. While the film shows zero resistance below T_C = 6.3 K, the onset T_C of

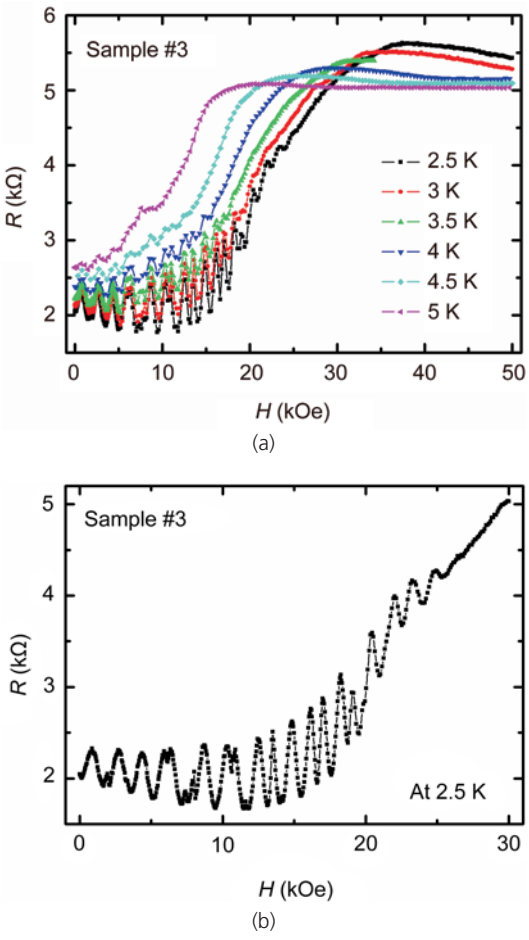

Figure 4 (a) Magnetoresistance of sample #3 with a magnetic field applied perpendicular to the film at different temperatures; (b) close-up view of (a) in the low magnetic field regime at 2.5 K for clarity

nanobridge sample #4 is at 6.7 K, which is higher than that of the film. Below T_C sample #4 exhibits residual resistance and strong quasi-periodic MR oscillations in the low field region, similar to sample #3. The R–H isotherms of sample #3 and #4 at 2.0 K in different magnetic field regimes are plotted in Fig. 6 for comparison. The oscillations of sample #3 with its larger residual resistance are stronger than those of sample #4. The MR oscillations are symmetric in positive and negative perpendicular fields. Although the dimensions of sample #3 and #4 are different, the periods of the oscillations are similar.

MR oscillations in superconducting amorphous and granular nanowires have previously been reported [23, 24]. In granular Sn nanowires [23], the MR oscillations near the superconductor–insulator (SI) transition were interpreted as an effect of screening currents circulating around phase

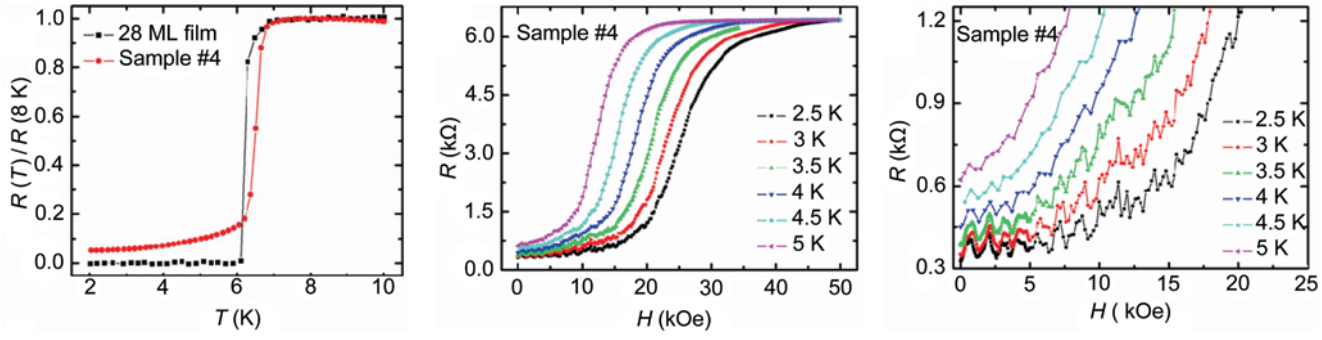

(a) (b) (c)

Figure 5 (a) Resistance vs temperature curves measured for a Pb film and a Pb bridge (sample #4). The film is 28 ML thick and used to make the 284 nm wide and 10 μm long Pb bridge (sample #4). (b) Magnetoresistance of sample #4 with a magnetic field applied perpendicular to the film at different temperatures. (c) Close-up view of (b) in the low magnetic field regime at different temperatures for clarity

coherent loops of weakly linked superconducting grains. In the case of amorphous indium oxide nanowires [24], the oscillations below T_C were explained by superconducting quantum interference device (SQUID)-like structures since the wires are not uniform in thickness. Recently, Xiao's group reported MR oscillations near T_C in a polycrystalline niobium nitride nanowire with a diameter of ~650 nm [25]. Their samples contained a high density of defects such as holes and gaps between grains and oscillations were observed from zero field to high field and were not periodic.

Our samples are single-crystalline bridges. The oscillations observed in samples #1–#4 only occured in the non-zero resistance region. In the magnetic-field-induced transition regions (non-zero resistance), all four samples showed MR oscillations. In the low field regime, samples #2–#4 exhibited residual resistance and MR oscillations were observed (see Fig. 3(f) and Figs. 4–6). Furthermore, the amplitude of the oscillations depends largely on the residual resistance. The larger the resistance is, the stronger are the oscillations. In contrast, sample #1 did not display any oscillations in the low field regime where the residual resistance $R = 0\ \Omega$ (see Fig. 3(c)). Therefore, the MR oscillations strongly depend on the inhomogeneous superconductivity, i. e., substantial normal regions of samples in the superconducting state.

Since the superconductivity in the bridges is

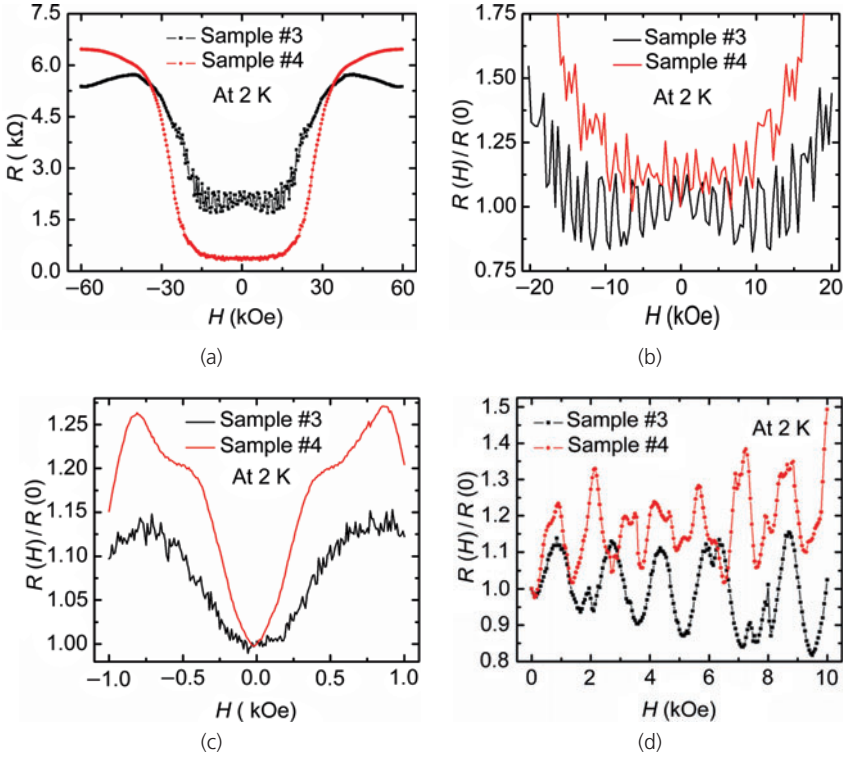

(a) (b) (c) (d)

Figure 6 (a) Magnetoresistance of samples #3 and #4 with a magnetic field applied perpendicular to the film at 2 K for comparison. (b) Close-up view of (a) in the low magnetic field regime at 2 K for clarity. The vertical scale is normalized to the resistance at zero field. (c) The symmetric magnetoresistance behavior of samples #3 and #4 at 2 K. The vertical scale is normalized to the resistance at zero field. (d) The magnetoresistance oscillations of samples #3 and #4 at 2 K for comparison. The vertical scale is normalized to the resistance at zero field

not homogeneous (non-zero resistance), possible superconducting ring-like structures [24] or superconducting Josephson junction arrays [26] may be responsible for the observed MR oscillations below T_C. The periods of the quasi-periodic oscillations of samples #1 and #2 are 394 Oe and 428 Oe. If we assume SQUID-type oscillations of two superconducting pathways separated by a normal or insulating region with an effective area $S=\phi_0/\Delta B$, where ϕ_0 is the flux quantum and ΔB is the period of the oscillations, we obtain areas of $S = 5.25 \times 10^{-14}$ m^2 for sample #1 and 4.83×10^{-14} m^2 for sample #2. Using the bridge length (2 μm) of samples #1 and #2, the two superconducting paths are separated by 26.3 nm in sample #1 and 24.2 nm in sample #2, which are roughly the same as the superconducting coherence lengths of the samples, 27.9 nm and 24.4 nm, respectively, estimated by $\xi \approx (\xi_0 l)^{1/2}$ [22]. If we assume the oscillations are from superconducting ring structures, according to $S=\pi d^2/4$, the diameter d is 259 nm in sample #1 and 248 nm in sample #2. The values are comparable to the width (350 nm) of samples #1 and #2. Since we did not study the samples when changing the bridge length while keeping the other parameters constant, it is hard for us to judge which mechanism for the observed MR oscillations is predominant. In addition, it is not easy to understand why we observed both non-periodic oscillations at low field and quasi-periodic oscillations in the transition region in sample #2. A very speculative explanation is that the influence from the 2-D films on both ends of the bridge cannot be neglected at low field. However, at high field (the field-induced transition region) the influence is suppressed or reduced.

3. Conclusions

We have investigated the transport properties of superconducting Pb nanobridges. Novel MR oscillations below T_C were observed. We attribute these to the inhomogeneous superconductivity in the bridges. Although some behavior is not well understood at present, the interesting phenomena reported here suggest that such Pb bridges can be a platform for studying the fundamental aspects of superconductivity in low dimensional regimes and may have promising applications in superconducting quantum interference devices [24, 27, 28]. We expect that our work will stimulate further experimental and theoretical interest.

Acknowledgements

We gratefully acknowledge technical support by Shao-Kui Su. We thank Dr. Lili Wang and Dr. Peng Jiang for their help in sample preparation. This work was financially supported by the National Science Foundation and the Ministry of Science and Technology of China and the Penn. State MRSEC under NSF grant DMR-0820404.

References

[1] Sharifi, F.; Herzog, A. V.; Dynes, R. C. Crossover from two to one dimension in *in situ* grown wires of Pb. *Phys. Rev. Lett.* **1993**, *71*, 428–431.

[2] Herzog, A. V.; Xiong, P.; Sharifi, F.; Dynes, R. C. Observation of a discontinuous transition from strong to weak localization in 1-D granular metal wires. *Phys. Rev. Lett.* **1996**, *76*, 668–671.

[3] Xiong, P.; Herzog, A. V.; Dynes, R. C. Negative magnetoresistance in homogeneous amorphous superconducting Pb wires. *Phys. Rev. Lett.* **1997**, *78*, 927–930.

[4] Bezryadin, A.; Lau, C. N.; Tinkham, M. Quantum suppression of superconductivity in ultrathin nanowires. *Nature* **2000**, *404*, 971–974.

[5] Camarota, B.; Parage, F.; Delsing, P.; Buisson, O. Experimental evidence of one-dimensional plasma modes in superconducting thin wires. *Phys. Rev. Lett.* **2001**, *86*, 480–483.

[6] Vodolazov, D. Y.; Peeters, F. M.; Piraux, L.; Mátéfi-Tempfli, S.; Michotte, S. Current–voltage characteristics of quasi-one-dimensional superconductors: An S-shaped curve in the constant voltage regime. *Phys. Rev. Lett.* **2003**, *91*, 157001.

[7] Tian, M. L.; Kumar, N.; Xu, S. Y.; Wang, J. G.; Kurtz, J. S.; Chan, M. H. W. Suppression of superconductivity in zinc nanowires by bulk superconductors. *Phys. Rev. Lett.* **2005**, *95*, 076802.

[8] Rogachev, A.; Bollinger, A. T.; Bezryadin, A. Influence of

high magnetic fields on the superconducting transition of one-dimensional Nb and MoGe nanowires. *Phys. Rev. Lett.* **2005**, *94*, 017004.

[9] Zgirski, M; Riikonen, K. -P.; Touboltsev, V.; Arutyunov, K. Size dependent breakdown of superconductivity in ultranarrow nanowires. *Nano Lett.* **2005**, *5*, 1029–1033.

[10] Altomare, F; Chang, A. M.; Melloch, M. R.; Hong, Y. G.; Tu, C. W. Evidence for macroscopic quantum tunneling of phase slips in long one-dimensional superconducting Al wires. *Phys. Rev. Lett.* **2006**, *97*, 017001.

[11] Guo, Y.; Zhang, Y. F.; Bao, X. Y.; Han, T. Z.; Tang, Z.; Zhang, L. X.; Zhu, W. G.; Wang, E. G.; Niu, Q.; Qiu, Z. Q.; Jia, J. F.; Zhao, Z. X.; Xue, Q. K. Superconductivity modulated by quantum size effects. *Science* **2004**, *306*, 1915–1917.

[12] Chiang, T. C. Superconductivity in thin films. *Science* **2004**, *306*, 1900–1901.

[13] Zhang, Y. F.; Jia, J. F.; Han, T. Z.; Tang, Z.; Shen, Q. T.; Guo, Y.; Qiu, Z. Q.; Xue, Q. K. Band structure and oscillatory electron-phonon coupling of Pb thin films determined by atomic-layer-resolved quantum-well states. *Phys. Rev. Lett*. **2005**, *95*, 096802.

[14] Bao, X. Y.; Zhang, Y. F.; Wang, Y. P.; Jia, J. F.; Xue, Q. K.; Xie, X. C.; Zhao, Z. X. Quantum size effects on the perpendicular upper critical field in ultrathin lead films. *Phys. Rev. Lett.* **2005**, *95*, 247005.

[15] Eom, D.; Qin, S.; Chou, M. -Y.; Shih, C. K. Persistent superconductivity in ultrathin Pb films: A scanning tunneling spectroscopy study. *Phys. Rev. Lett.* **2006**, *96*, 027005.

[16] Ozer, M. M.; Thompson, J. R.; Weitering, H. H. Hard superconductivity of a soft metal in the quantum regime. *Nat. Phys.* **2006**, *2*, 173–176.

[17] Wang, J.; Ma, X. C.; Qi, Y.; Fu, Y. S.; Ji, S. H.; Lu, L.; Jia, J. F.; Xue, Q. K. Negative magnetoresistance in fractal Pb thin films on Si(111). *Appl. Phys. Lett.* **2007**, *90*, 113109.

[18] Wang, J.; Ma, X. C.; Qi, Y.; Fu, Y. S.; Ji, S. H.; Lu, L.; Xie, X. C.; Jia, J. F.; Chen, X.; Xue, Q. K. Unusual magnetoresistance effect in the heterojunction structure of an ultrathin single-crystal Pb film on silicon substrate. *Nanotechnology* **2008**, *19*, 475708.

[19] Rogachev, A.; Bezryadin, A. Superconducting properties of polycrystalline Nb nanowires templated by carbon nanotubes. *Appl. Phys. Lett.* **2003**, *83*, 512–514.

[20] Tian, M. L.; Wang, J. G.; Kurtz, J. S.; Liu, Y.; Chan, M. H. W. Dissipation in quasi-one-dimensional superconducting single-crystal Sn nanowires. *Phys. Rev. B* **2005**, *71*, 104521.

[21] Shanenko, A. A.; Croitoru, M. D.; Zgirski, M.; Peeters, F. M.; Arutyunov, K. Size-dependent enhancement of superconductivity in Al and Sn nanowires: Shape-resonance effect. *Phys. Rev. B* **2006**, *74*, 052502.

[22] Wang, J.; Ma, X. C.; Lu, L.; Jin, A. Z.; Gu, C. Z.; Xie, X. C.; Jia, J. F.; Chen, X.; Xue, Q. K. Anomalous magnetoresistance oscillations and enhanced superconductivity in single-crystal Pb nanobelts. *Appl. Phys. Lett.* **2008**, *92*, 233119.

[23] Herzog, A. V.; Xiong, P.; Dynes, R. C. Magnetoresistance oscillations in granular Sn wires near the superconductor–insulator transition. *Phys. Rev. B* **1998**, *58*, 14199–14202.

[24] Johansson, A.; Sambandamurthy, G.; Shahar, D.; Jacobson, N.; Tenne, R. Nanowires acting as a superconducting quantum interference device. *Phys. Rev. Lett.* **2005**, *95*, 116805.

[25] Patel, U.; Avci, S.; Xiao, Z. L.; Hua, J.; Yu, S. H.; Ito, Y.; Divan, R.; Ocola, L. E.; Zheng, C.; Claus, H.; Hiller, J.; Welp, U.; Miller, D. J.; Kwok, W. K. Synthesis and superconducting properties of niobium nanowires and nanoribbons. *Appl. Phys. Lett.* **2007**, *91*, 162508.

[26] Van der Zant, H. S. J., Webster, M. N., Romijn, J.; Mooij, J. E. Vortices in two-dimensional superconducting weakly coupled wire networks. *Phys. Rev. B* **1994**, *50*, 340–350.

[27] Hopkins, D. S.; Pekker, D.; Goldbart, P. M., Bezryadin, A. Quantum interference device made by DNA templating of superconducting nanowires. *Science* **2005**, *308*, 1762–1765.

[28] Pekker, D.; Bezryadin, A.; Hopkins, D. S.; Goldbart, P. M. Operation of a superconducting nanowire quantum interference device with mesoscopic leads. *Phys. Rev. B* **2005**, *72*, 104517.